ANNUAL REPORT

NASA CONTRACT NO. S-49296(G)

MEASUREMENT OF THE VELOCITY OF LIGHT

FACILITY FORM 602

N66-13647 (ACCESSION NUMBER) (THRU) 1

51 (PAGES) (CODE) 23

CR 68779 (NASA CR OR TMX OR AD NUMBER) (CATEGORY)

GPO PRICE $ _____

CFSTI PRICE(S) $ _____

Hard copy (HC) 3.00

Microfiche (MF) .50

ff 653 July 65

ANNUAL REPORT

NASA Contract No. S-49296(G)

Measurement of the Velocity of Light

I. INTRODUCTION

Recent developments in different fields of experimental research make it appear possible to measure the velocity of light with an accuracy surpassing that of previous measurements by several orders of magnitude. The present probable error is about 3 parts in 10^7.

1) Continuously operated (CW) gas lasers provide for radiation sources which under proper conditions can achieve linewidths of a few Hz, short term stability of the order 5 kHz and wavelength resettability of a part in 10^9 [1,2].

2) The technique of optical cavities (Fabry-Perot interferometers) has progressed so far that interferometers of a few meters length can be made with a finesse of a few 100 [3].

3) Detailed calculations indicate[4] that by the use of a traveling wave photocathode ray tube optical beat frequencies up to 10^{12} Hz can be accurately measured, provided the response time of composite photocathodes is significantly shorter than 10^{-12} sec.

With the use of the above techniques the velocity of light can be measured with a precision of about 1 part in 10^9 or better when an interferometer of one to two meters is used. It must be emphasized that the above precision corresponds to limitations inherent in the equipment,

while the accuracy of the measurement is limited by the present length standard. The accuracy of the presently accepted Kr^{86} wavelength standard is about 1 part in 10^8. A factor five improvement could be made using a Hg^{198} wavelength standard. Because of these limitations imposed by the length standard, efforts aiming at higher accuracy are meaningless unless a new length standard is developed.

Outline of the Velocity of Light Measurement

The measurement of c is based on the

1) Measurement of the beat frequency, $\nu_1-\nu_2$, between two laser lines, and on the

2) Simultaneous measurement of the wave number difference k_1-k_2, between the same two laser lines.[4]

The basic equation to obtain c is

$$\nu_1-\nu_2 = c\left(\frac{1}{\lambda_1}-\frac{1}{\lambda_2}\right) = c(k_1-k_2) \qquad 1$$

$$c = \frac{\nu_1-\nu_2}{k_1-k_2} \qquad 2$$

and the relative accuracy in c is

$$\frac{\delta c}{c} = \frac{\delta(\nu_1-\nu_2)}{\nu_1-\nu_2} + \frac{\delta(k_1-K_2)}{k_1-k_2} \qquad 3$$

An important conclusion can be drawn from Eq. 2. If the beat frequency, $\nu_1-\nu_2$, is maintained constant in the experiment, k_1-k_2, the wave number difference to be measured, is also a constant. Thus, efforts in the experi-

ment should be directed toward stabilizing the light source to a constant beat frequency and measuring the corresponding constant difference of the wave numbers, rather than the wave numbers themselves.

A second important conclusion is that if ν_1 and ν_2 are generated in the same laser cavity, the fluctuations in $\nu_1-\nu_2$ and, therefore, k_1-k_2 are correlated, thus,

$$\frac{\delta(\nu_1-\nu_2)}{\nu_1-\nu_2} \simeq \frac{\delta\nu_1}{\nu_1} = \frac{\delta\nu_2}{\nu_2}$$

and

$$\frac{\delta(k_1-k_2)}{k_1-k_2} \simeq \frac{\delta k_1}{k_1} = \frac{\delta k_2}{k_2}$$

or

$$\delta(\nu_1-\nu_2) \simeq \frac{\nu_1-\nu_2}{\nu_1}\,\delta\nu_1$$

and

$$\delta(k_1-k_2) \simeq \frac{k_1-k_2}{k_1}\,\delta k_1$$

This correlation reduces the requirement of the absolute stability of the laser lines and is of fundamental importance in obtaining the desired precision in the measurement of $\underline{c}$.

II. DETERMINATION OF k_1-k_2.

The total uncertainty in the measurement of (k_1-k_2) is

$$\frac{\delta(k_1-k_2)}{k_1-k_2} = \sqrt{2}\frac{dk}{k} + \frac{\delta L}{L} + \frac{q}{LF(k_1-k_2)}$$

where the first term on the right represents the relative fluctuation of the correlated laser lines k_1 and k_2 and the last two terms represent fluctuations in the interferometer used to measure (k_1-k_2). F represents the finesse of the interferometer and q is a measure of that fraction of the finesse curve that can be reproducibly determined. By taking full advantage of the correlated fluctuations of k_1-k_2 resulting from fluctuation in the laser and the passive Fabry-Perot, a direct measurement of k_1-k_2 could be made with a precision approaching 1 part in 10^{11} based on the expected signal to noise ratio. The accuracy of the measurement of k_1-k_2 therefore depends on limitations imposed by systematic errors.

In addition to the errors discussed above, we must consider the error involved in the diffraction phase shift associated with the measurement of k_1-k_2 and errors due to irregularities in the mirrors. These effects are currently under theoretical and experimental study in order to more precisely determine the nature of these errors.

III. BEAT FREQUENCY DETECTION:

In addition to the measurement of the wave number separation k_1-k_2, the beat frequency $\nu_1-\nu_2 = c(k_1-k_2)$ must be accurately determined. The

details of the frequency measurement procedure are given in Appendix I and will be outlined here.

We consider a photocathode-ray tube with a serpentine traveling wave deflection system. The two frequencies ν_1 and ν_2 having a frequency stability of 5 kHz strike the photocathode. Because the photocathode is a square law detector the number of photoelectrons emitted is proportional to

$$E^2 = (E_1+E_2)^2 = E_1^2+E_2^2+ 2E_1 \cdot E_2$$

When E^2 is time averaged over an optical period, and $E_1 = E_2 = E_o$,

$$\overline{E^2} = E_o^2 \left\{1+ \cos\left[2\pi(\nu_1-\nu_2)t+\varphi\right]\right\}$$

where $(\nu_1-\nu_2) \simeq 10^{12}$ Hz. The modulated electron beam is then accelerated and enters a traveling wave serpentine deflection system operating at a frequency $\Omega \simeq 10^{10}$ Hz and is focused on a fluorescent screen. Since the electrons are modulated at a frequency $(\nu_1-\nu_2)$ and deflected at a frequency Ω the resulting pattern on the screen is a series of n dots, where

$$n = \frac{\nu_1-\nu_2}{\Omega}$$

If n is an integer the dot pattern will be standing, otherwise, it is a running pattern. Such a running pattern can be viewed through a screen which has n_o openings where n_o is an integer, say the nearest integer to

$\nu_1-\nu_2/\Omega$. The running dot pattern can then be detected with a photomultiplier at a frequency

$$\pm\mu = n_o\,\Omega - (\nu_1-\nu_2)$$

By measuring the frequencies μ and Ω, and knowing n_o, the photobeat $(\nu_1-\nu_2)$ can be determined. Detailed calculations in Appendix I show that $(\nu_1-\nu_2)$ can be determined unambiguously by sweeping Ω over $\sim$ 1% of its central value.

The expected accuracy of the measurement of $\nu_1-\nu_2$ is shown in Appendix I to be of the order 1 part in 10^{10}. Since ν_1 and ν_2 come from the same laser, the uncertainty in $\nu_1-\nu_2$ is

$$\delta(\nu_1-\nu_2) = \frac{(\nu_1-\nu_2)\delta\nu}{\nu_1}$$

If $\nu_1 \simeq 3\times10^{14}$ Hz, $\nu_1-\nu_2 \simeq 10^{12}$ Hz, and $\delta\nu_1$ 15 kHz, then

$$\delta(\nu_1-\nu_2) \simeq 50 \text{ Hz}$$

Here we again see the importance of the correlated fluctuations of ν_1 and ν_2 when they are derived from the same laser cavity. The frequency Ω has a stability exceeding 1 part in 10^{10} and will be discussed below. μ can be measured with an accuracy of $\pm$ 1 Hz so that $(\nu_1-\nu_2)$ should be accurately known to 1 part in 10^{10} or better.

IV. EXPECTED ACCURACY

The uncertainty in the measurement of the velocity of light is given by

$$\frac{\delta c}{c} = \frac{\delta(\nu_1-\nu_2)}{\nu_1-\nu_2} + \frac{\delta(k_1-k_2)}{k_1-k_2}$$

The uncertainty in the measurement of $\nu_1-\nu_2$ is expected to be 1 part in 10^{10} as discussed in Section III and Appendix I.

The uncertainty in the measurement of k_1-k_2 is discussed in Section II. It is expected that this uncertainty will be limited by systematic errors such as the errors involved in the diffraction phase shift correction for k_1-k_2 or in mirror irregularities. It is reasonable to expect that the accuracy in the determination of k_1-k_2 could approach 1 part in 10^{10}.

The most serious restriction on the accuracy of the c measurement is the limitation of the currently accepted length standard. The wavelength of either λ_1 or λ_2 must be compared with the Kr^{86} wavelength standard and the accuracy of this determination is limited to one part in 10^8. Any greater accuracy than this means that a length standard differing from the internationally accepted one be used. Standards reproducible to better than 2 parts in 10^9 have yet to be developed. It may be desirable to regard the measurement described above as a new length standard if other approaches do not prove fruitful.

Progress Report

A High Frequency Phototube

The photocathode-ray tube which is to be used in the measurement of the terahertz photobeat is being constructed on a contractual basis by Edgerton, Germeshausen & Grier, Inc. located in Bedford, Massachusetts. The current status of the phototube is that a prototype is to be delivered on or about August 1, 1965. Several technical difficulties involving the photocathode deposition and deflection system alignment have occurred and have been eliminated.

B 10 Gc Deflection System Power Supply:

The 10 Gc/s deflection system power supply has been completed, tested, and delivered. The system has been checked for phase, frequency, and power stability and has met all the specifications required for operating the deflection system of the phototube such that the accuracy of the driving system frequency is better than 1 part in 10^{10} at an output power of 500 watts. Figure 1 shows the deflection system power supply apparatus.

C Stability of the lasers

It was stated in section III of this report that with a stability of 15 kHz for ν_1 and ν_2, $\nu_1-\nu_2$ has a stability of $\simeq$ 50 Hz. It is therefore necessary to show, that this stability exists. Figure 2 shows a photograph of a sound shielded room in which two 1 meter internal mirror lasers are mounted on an isolated table. The free running stability of these lasers is determined by photomixing the single mode output at an approximate 1 mHz offset and looking at the frequency spectrum of the photobeat.

Figure 3 shows typical frequency spectra of the beat note which indicates that the short term (1 sec) free running stability of the lasers is between 15 and 50 kHz. It is important to note that the independent fluctuation rate of the two lasers is less than 3 kHz and that the output is virtually free of fluctuations when the beat frequency is observed in a time comparable to this rate. The observed fluctuation and fluctuation rate should be adequate for the preliminary investigation of the high frequency photobeats.

A more serious consideration is the long term stability of the lasers. In order to insure that the laser lines do not drift over a large frequency range in a period of an hour or longer, one must stabilize the laser cavity to some characteristic point on the atomic transition. Such a characteristic point is the center of the "Lamb dip" which is shown in figure 4 which is a graph of the output power as a function of the frequency difference $(\nu_L-\nu_c)$ where ν_L is the laser frequency and ν_c is the frequency of the center of the atomic line center of the laser transition. One can also use the dispersion of the "Lamb dip" in order to set to the center of the laser transition. The dispersion is obtained by modulating the inversion density of one laser. The output is observed by photomixing the output of this laser with a second laser which is slaved at a 10.7 mHz offset. The details of this technique are given in Appendix II for the 1.15μ neon transition. An error signal can be developed by phase detecting the frequency modulated output resulting from the modulation of the inversion density which is used to stabilize the laser to the line center. The

advantage of this method of stabilization is that the output of the slaved laser, locked 10.7 mHz from the line center, is constant in amplitude and frequency.

This locking technique has been used to stabilize the output of a pair of lasers with a long term stability of 1 mHz.

D 30 Meter Interferometer

About the same time that development of the photocathode-ray tube was started, work was also begun on the construction of a 30 meter long vacuum Fabry-Perot interferometer. A location in an unused mine about five miles west of Boulder was chosen in order to minimize man-made disturbances and to maximize the thermal stability. Construction of the interferometer was started: a) to make sure that a substantially improved speed of light measurement can be achieved even if some unexpected limitation such as a significant time spread in the photocathode emission should prevent the detection of beat frequencies approaching 10^{12} Hz with the photocathode-ray tube; and b) to investigate the systematic errors involved in measuring k_1-k_2 in order to help in determining whether, for a beat frequency of about 10^{12} Hz, a substantially better measurement can be made with the 30 meter interferometer than with a considerably shorter device. Because of the supporting nature of the long interferometer part of the speed of light project, it is being carried out with a considerably lower level of effort than the high frequency phototube part. A large amount of the work has been done by University of Colorado graduate students.

For a long interferometer it seemed difficult to mount the end mirrors from a spacer which is isolated from the earth as is usually done for one or two meter interferometers. Instead, piers to hold mirrors have been installed in holes drilled in the granite floor of the mine tunnel at each en end of the path. The vacuum boxes mounted on the piers are isolated from the pipes connecting the boxes by flexible bellows. With this arrangement the stability of the mirror separation is determined mainly by the stability of the rock. Known sources of fluctuations in the pier separation are: a) microseisms caused by storms in the oceans which give variations at frequencies of roughly 0.1 to 10 Hz with an expected amplitude of about 1 part in 10^{10} in Colorado: b) rock tides (also called solid earth tides) caused by the moon and having a 12 hour period and an amplitude of roughly 5 parts in 10^{9}.

Preliminary measurements with the 30 meter vacuum Fabry-Perot interferometer have been made using temporary mirrors of 1/20 wavelength quality and 50 meter radius of curvature. 6328 A light from a helium-neon laser was approximately matched into the axial modes of the interferometer and fringes were observed in the transmitted light by modulating the laser frequency at several hundred Hz. The observed finesse was about 30, corresponding to an interferometer mode width of about 150 kHz. Useful measurements of the path stability have not yet been possible because the laser used so far has some air in the path between the mirrors and is therefore subject to frequency fluctuations as the atmospheric density changes. However, the observed short term fluctuations in the fringe position are consistent with the expected microseism amplitude.

Plans for next Contract Period

A) High Frequency Phototube

The schedule for the next contract period is as follows:

1) It is expected that an experimental investigation to detect laser beat frequencies will begin immediately and that preliminary results of this investigation shall be obtained by January 1, 1966.

2) Assuming that the laser photobeat experiment is successful, a preliminary measurement of the wave number separation of the two laser lines will be made. At the same time, investigation of the diffraction phase shift corrections will be pursued.

B) 30 Meter Interferometer

During the next year we hope to make measurements of the path stability by locking the laser to a stable 30 cm interferometer located in the vacuum and then observing changes in the long path fringe position. We also plan to measure the whole fringe number for the long path by the technique of optical multiplication. Hopefully, results with the High Frequency Phototube will be available by the end of the year and will make possible a decision on whether to speed up work on the long path.

References

1) A. Javan, W. R. Bennett, Jr., and D. R. Herriot, Phys. Rev. Letters 6, 106, 1961.

2) T. S. Jaseja, A. Javan, and C. H. Townes, Phys. Rev. Letters 10, 165, 1963.

3) R. A. Paananen, Proc. IRE 50, 2115, 1962.

4) Z. Bay and H. S. Boyne, Rendiconti S.I.F. Corso 31, August 1963 Academic Press New York 1964 (Included as Appendix I).

APPENDIX I

The Use of Terahertz Photobeats for Precise Velocity-of-Light Measurements.

Z. BAY and H. S. BOYNE

Atomic Physics Division, National Bureau of Standard - Washington, D. C.

Estratto da *Rendiconti della Scuola Internazionale di Fisica «E. Fermi»* - XXXI Corso

1. – Introduction.

The coherent output from a continuous He-Ne gas laser [1] can be used as a radiation source for the development of long-range interferometry. Interferometer fringes have already been obtained for optical path differences up to 200 m [2]. The experimental results of Javan indicate that with sufficient mechanical and thermal isolation one can achieve linewidths of a few Hz, stability of the order 5 kHz and wavelength resettability of a part in 10^9 [3]. With such a source, the limitations of any interferometric study are instrumental.

Because of the coherence of the laser radiation it is possible to measure accurately the beat frequency between two laser lines using photomixing techniques [4]. Detailed calculations presented below show that by the use of a traveling-wave cathode-ray tube beat frequencies up to the order of 10^{13} Hz can be accurately measured. With the interferometric study of the corresponding wave-number difference a precision of one part in 10^8 for the velocity of light could be achieved with a path length of a few meters.

2. – General description.

The experimental involves measuring the wavelength of a stabilized He-Ne laser with respect to the wavelength standard, measuring the difference in wavelength between two laser lines, and measuring the difference in frequency between the same two laser lines. If we have two lines which are closely

spaced, λ_1 and λ_2, the frequency and wavelength in vacuum are given by

$$\nu_1 = c/\lambda_1 , \qquad \nu_2 = c/\lambda_2 ,$$

therefore

$$\nu_2 - \nu_1 = c\left[\frac{1}{\lambda_2} - \frac{1}{\lambda_1}\right] = \Delta\nu$$

or

$$\Delta\nu = c\,\frac{\Delta\lambda}{\lambda_1\lambda_2}$$

and

$$c = \frac{\Delta\nu}{\Delta\lambda}\,\lambda_1\lambda_2$$

or

$$c = \frac{\Delta\nu}{\Delta\lambda}\,\lambda_1(\lambda_1 - \Delta\lambda) . \tag{1}$$

This is the basic equation in which λ_1, $\Delta\lambda$, and $\Delta\nu$ are to be determined. It will be more convenient to express eq. (1) in terms of the beat frequency $\Delta\nu = \omega$ and the wave number separation $K = k_1 - k_2$ where $k = 1/\lambda$. Therefore,

$$c = \omega/K . \tag{2}$$

The uncertainty in the measurement of c is given by

$$\frac{\partial c}{c} = \frac{\partial\omega}{\omega} + \frac{\partial K}{K} .$$

The uncertainty of K is discussed in the next Section. The uncertainty with which one can measure ω will be discussed in Sect. **6**.

3. – Wavelength measurement.

We wish to consider an evacuated Fabry-Perot scanning interferometer for the measurement of K. The difference $\lambda_1 - \lambda_2$ would be measured with linear scanning techniques which have been used successfully in the measurements of isotope shifts and in the comparison of spectral lines with the krypton standard. The linear scan could be accomplished with magnetostrictive invar spacers, or by changing the index of refraction in a linear manner [5].

The uncertainty in the measurement of λ_1 with respect to the length standard depends, of course, on what is used as the wavelength standard. If λ_1 is determined with respect to the krypton standard, an uncertainty in the measurement of 1 part in 10^8 is expected [6]. The precision with which one can measure $\Delta\lambda = \lambda_1 - \lambda_2$ depends on the spectral range and the finesse of the interferometer.

The instrumental linewidth of a Fabry-Perot interferometer is given in cm^{-1} by $\Delta = 1/2LF$ where L is the spacer length and F is the finesse. If $\mathscr{E}$ represents that fraction of the linewidth which can be determined reproducibly, the uncertainty in determining K is $\delta K = \mathscr{E}\Delta$. Therefore

$$\frac{\delta K}{K} = \frac{\mathscr{E}}{2FLK} = c\frac{\mathscr{E}}{2FL\omega}. \tag{3}$$

One sees from eq. (3) that:

1) For given values of $\delta K/K$, F, and $\mathscr{E}$ the precision of the measurement is determined by the product $L\omega$. Therefore, the higher ω is, the smaller L has to be. For example, if $\delta K/K = 10^{-8}$, $F = 100$, and $\mathscr{E} = 0.01$ in the region from 1.0 μm to 1.2 μm [7], then for $\omega = 10^{10}$ Hz, L must be 150 meter whereas, for $\omega = 10^{12}$ Hz, $L = 1.5$ meter.

2) For given values of L, F, and $\mathscr{E}$ the precision of the c measurement increases in proportion to the beat frequency ω.

We shall therefore attempt to measure the highest beat frequencies possible (*i.e.* 10^{12} Hz). The laser lines of interest in the He-Ne system are listed in the following table [8]:

Laser lines (μm)	K (cm^{-1})	ω ($\cdot 10^{12}$ Hz)
1.207 1.199	58	1.66
1.084 1.080	40	1.2
1.118 1.115	28	0.83
1.141 1.139	14.4	0.43
1.161 1.160	9.3	0.28

4·1. *Frequency measurement.* – The measurement of a 10^{12} Hz beat frequency requires means exceeding common techniques. The frequency range is a factor 50 greater than frequencies which have been measured with photosurfaces to date [4] and is considerably beyond the present capabilities of microwave technology. We wish to examine in detail the possibility of measuring such frequencies using traveling-wave cathode-ray tube techniques.

Basically, the measurement is visualized in the following way. The two laser lines of interest with electric field strengths

$$E_1 = E_0 \cos(2\pi\nu_1 t + \varphi),$$

$$E_2 = E_0 \cos(2\pi\nu_2 t),$$

are focused on a photocathode. Since the photocathode is a square-law detector, the number of photoelectrons emitted per unit time is proportional to

$$E^2 = (E_1 + E_2)^2 = E_1^2 + E_2^2 + 2E_1 \cdot E_2$$

or

$$E^2 = E_0^2\{\cos^2(2\pi\nu_1 t + \varphi) + \cos^2 2\pi\nu_2 t + \\ + \cos[2\pi(\nu_1 - \nu_2)t + \varphi] + \cos[2\pi(\nu_1 + \nu_2)t + \varphi]\}.$$

The optical frequencies ν_1 and ν_2 are $\sim 3\cdot 10^{14}$ Hz and the beat frequency $\nu_1 - \nu_2 \simeq 10^{12}$ Hz. If E^2 is time-averaged over an optical period then [9]

$$\overline{E^2} = E_0^2\{1 + \cos[2\pi(\nu_1 - \nu_2)t + \varphi]\} = E_0^2\{1 + \cos(2\pi\omega t + \varphi)\} \tag{4}$$

and $\overline{E^2}$ is 100% modulated (assuming equal amplitudes E_0 of electric fields E_1 and E_2). The modulated electron beam is now accelerated and enters into a traveling-wave deflection system operating at the driving frequency $\Omega \simeq 10^{10}$ Hz and is then focused on a fluorescent screen. Since the electron

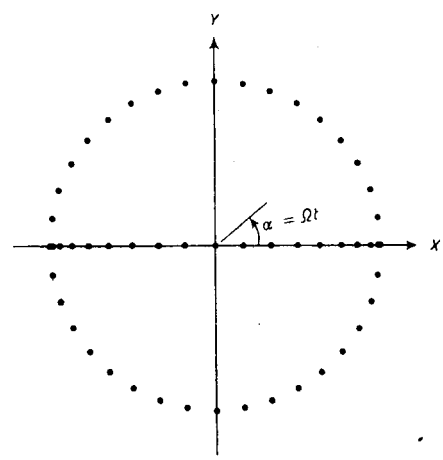

Fig. 1. – Schematic representation of the intensity-modulated cathode-ray spot. The dots along the x-axis represent the projection of the circular dot pattern.

beam is modulated at frequency ω and deflected at frequency Ω, the resultant display on the screen will be intensity modulated.

In the ideal case of appropriately phased simutaneous X and Y deflection, the cathode ray spot on the screen moves on a circle with frequency Ω (see Fig. 1). Because of the intensity modulation of the beam at frequency ω, there will be $\omega/\Omega = n$ light spots on the screen. If n is an integer the spot pattern is standing, otherwise it runs around the circle. Such a running pattern can be viewed through a mask which has n openings where n is an integer, say the nearest integer to ω/Ω. The number n will be referred to as the mask number.

Consider a mask made as a film with a transmission for light (from a fluorescent screen)

$$\varrho = \tfrac{1}{2}(1 + \cos n\alpha)\,, \tag{5}$$

where α is the polar angle around the center of the circle (Fig. 1). Such a mask will multiply the sweep frequency Ω by n. With no electron-beam modulation ($\omega = 0$), a photocell mounted to view the total fluorescent light intensity from the pattern through the mask would, in principle, have a response at the frequency $n\Omega$. When the electron beam is modulated according to eq. (4) the total light intensity seen through the mask is

$$\begin{aligned} I = \tfrac{1}{2} I_0[1 + \cos(2\pi\omega t + \varphi)][1 + \cos 2\pi n\Omega t] = \\ = \tfrac{1}{2} I_0\{1 + \cos(2\pi\omega t + \varphi) + \cos 2\pi n\Omega t + \\ + \tfrac{1}{2}\cos[2\pi(\omega + n\Omega)t + \varphi] + \tfrac{1}{2}\cos[2\pi(\omega - n\Omega)t + \varphi]\}\,. \end{aligned}$$

This expression must now be averaged over a time equal to the response time of the fluorescent screen which is much longer than the period $1/\omega$ but shorter than the period $1/(\omega - n\Omega)$. Therefore, all oscillatory terms except the last term will average to zero and

$$\bar{I} = \tfrac{1}{2} I_0\{1 + \tfrac{1}{2}\cos[2\pi(\omega - n\Omega)t + \varphi]\}\,. \tag{6}$$

If $\omega - n\Omega = 0$ the pattern is standing and the intensity can be anything between $\frac{1}{4} I_0$ and $\frac{3}{4} I_0$ depending on the value of the phase constant φ. If $\omega - n\Omega \neq 0$, $\bar{I}$ oscillates with a frequency

$$\pm\mu = \omega - n\Omega\,.$$

Since the mask number n is a fixed parameter chosen for the experiment, ω can be determined by measuring μ and Ω.

In the proposed measurement it is assumed that $\omega \sim 10^{12}$ Hz, $n = 100$, $\Omega \sim 10^{10}$ Hz can be varied over $\sim 1\%$ of its center frequency so that the frequency μ (e.g., 10^{7} Hz) can be fixed by applying a narrow band filter to the output of the photomultiplier. In this case there are two values of Ω for which the filter responds:

$$n\Omega_+ = \omega + \mu\,, \qquad n\Omega_- = \omega - \mu\,.$$

Therefore

$$\omega = n\bar{\Omega} = n\left[\frac{\Omega_+ + \Omega_-}{2}\right] \tag{7}$$

and

$$\Omega_+ - \Omega_- = 2\frac{\mu}{n}\,. \tag{8}$$

Measurement of Ω_+ and Ω_- for a fixed frequency μ determines ω unambigously.

It must be noted that the appearance of a unique doublet is bound to the conditions of the ideal experiment, that is, pure harmonic modulation of the beam and pure harmonic transparency of the mask. Departures from ideal conditions of modulation are discussed in the Appendix.

It is interesting to point out that in the measurement of the frequency μ the current of the photomultiplier is integrated over the response time of the low-frequency filter. This charge-accumulating feature of the experiment helps decisively in improving the signal-to-noise ratio appearing in the output, as compared to that existing in the photocurrent of the cathode-ray tube. For a photocurrent of 10^{10} electrons/s, there is on the average only 1 photoelectron appearing in the period of 100 beats while the relative fluctuation in the output current, with a filter bandwidth of $\sim 10^{3}$ Hz, is only ~ 3 parts in 10^{4} (cf. Sect. 6).

4·2. *Application to one-deflection system.* – In the proposed experiment the deflection will be restricted to one dimension (call it X) therefore the circular motion of the spot must be projected on the X axis (Fig. 1)

$$X = R\cos\alpha\,, \qquad \alpha = \cos^{-1}\frac{X}{R}\,. \tag{9}$$

The mask is now aligned along the X axis and its transparency ϱ is a function of X

$$\varrho = \frac{1}{2}\left[1 + \cos n\left\{\cos^{-1}\frac{X}{R}\right\}\right] \tag{10}$$

Fig. 2. – Mask used in the model experiment. The mask was made from a photograph of a standing-dot pattern by modulating the beam of a Tektronix Model 533 cathode-ray tube at the frequency $\omega = 10^5$ Hz and deflecting the beam at the frequency $\Omega = 10^3$ Hz. The mask number is $n = 100$.

representing a wave structure in which the waves are compressed at each end (Fig. 1 and 2). Since in a full sweep period (α changing from 0 to 2π) the beam spot passes twice along the mask, the number of waves in the mask is $n/2$. It is reasonable now to choose n as an even integer in order to avoid half-waves in the mask. It is also desirable to make the transparency function symmetric around the center of the mask. This condition is satisfied if the mask number n is a multiple of 4.

5. – Analysis of cathode-ray-tube response.

Thus far, we have assumed that the response of the photocathode of the tube is sufficiently fast to modulate the electron beam with frequencies up to 10^{12} Hz. We now wish to analyse this problem in detail.

5·1. *Correlation time of the electron-photon interaction.* – PERSHAN and BLOEMBERGEN [10] have estimated this interaction time in metals to be of order $\tau = 10^{-14}$ second at room temperature. This means that modulations (beats) in the light intensity can be detected up to $1/\tau = 10^{14}$ Hz. Corresponding interaction times are not known for composite photolayers (Ag-O-Cs cathode) but we shall assume them to be similar to the above figure for pure metals. Therefore we do not expect the electron-photon interaction time to be a limitation in this experiment.

5·2. *Transit-time spread in the photolayer.* – If there is no delay due to electron scattering within the lattice, the electron which absorbs 1 eV inside the layer must traverse a typical layer thickness for the photocathode of 150 Å in the time

$$t = \frac{X}{v} = \frac{150 \cdot 10^{-8} \text{ cm}}{5 \cdot 10^7 \text{ cm/s}} \simeq 3 \cdot 10^{-14} \text{ s} .$$

This transit time will have a spread since the electrons are not all traveling normal to the surface and not all electrons traverse the full thickness of the layer. However, the average spread can be expected to be less than 10^{-13} second which would represent an upper frequency limit in this measurement of 10^{13} Hz.

5·3. *Velocity spread of photoelectrons.* – There is an energy distribution of electrons emitted from the photocathode which causes a spread in the electron bunching and reduces the percentage modulation. We shall assume that the energy distribution of photoelectrons emerging from composite photocathodes is similar to the distribution for the alkali metals. Since we are interested in the normal energy distribution in the vicinity of maximum energy, we shall use the theory of DU BRIDGE [11] which applies to this situation for pure metals and is confirmed by precise experiments on potassium [12]. The maximum energy attainable is given by

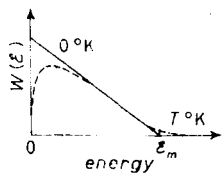

Fig. 3. – Normal energy distribution of emitted photoelectrons according to DuBridge's theory. The solid line represents the distribution at 0° K. The dashed line indicates the distribution at room temperature.

$$\mathscr{E}_m = h\nu - \Phi e \,,$$

where Φ is the work function. In our case $h\nu \sim 1$ eV and $\Phi \simeq \frac{3}{4}$ V [13] thus $\mathscr{E}_m \simeq \frac{1}{4}$ eV. We take the distribution of « normal energies » which is a linear curve at 0 °K with the peak at zero energy. At room temperature the maximum of the distribution is shifted to slightly higher energies (Fig. 3). Since the half width of the energy distribution curve is about the same at absolute zero and at room temperature the absolute-zero distribution will be used in order to facilitate calculations.

The linear energy distribution function is

$$W(\mathscr{E}) = \frac{2}{\mathscr{E}_m^2}(\mathscr{E}_m - \mathscr{E}) \,. \tag{11}$$

The velocity distribution is obtained from the energy distribution

$$\varphi(v)\,\mathrm{d}v = W(\mathscr{E})\,\mathrm{d}\mathscr{E}$$

and $\frac{1}{2}Mv^2 = \mathscr{E}$, where M is the electron mass:

$$\varphi(v) = 4/v_m^4[v_m^2 v - v^3] \,. \tag{12}$$

The problem of spread will now be analysed on the energy scale and the velocity scale.

1) Energy scale:

$$\bar{\mathscr{E}} = (2/\mathscr{E}_m^2)\int_0^{\mathscr{E}_m} (\mathscr{E}\mathscr{E}_m - \mathscr{E}^2)\,\mathrm{d}\mathscr{E} = 1/3\mathscr{E}_m \,, \tag{13}$$

$$\overline{\mathscr{E}^2} = (2/\mathscr{E}_m^2)\int_0^{\mathscr{E}_m} (\mathscr{E}^2\mathscr{E}_m - \mathscr{E}^3)\,\mathrm{d}\mathscr{E} = 1/6\mathscr{E}_m^2\,, \tag{14}$$

$$\Delta\mathscr{E}^2 = [\overline{\mathscr{E}^2} - (\overline{\mathscr{E}})^2] = (\tfrac{1}{6} - \tfrac{1}{9})\mathscr{E}_m^2 = \tfrac{1}{18}\mathscr{E}_m^2 \tag{15}$$

and

$$\text{r.m.s. } \Delta\mathscr{E} \simeq \tfrac{1}{4}\mathscr{E}_m\,. \tag{16}$$

2) Velocity scale:

$$\bar{v} = (4/v_m^4)\int_0^{v_m} (v_m^2 v^2 - v^4)\,\mathrm{d}v = 4(1/3 - 1/5)v_m = (8/15)\,v_m\,, \tag{13a}$$

$$\overline{v^2} = (4/v_m^4)\int_0^{v_m} (v_m^2 v^3 - v^5)\,\mathrm{d}v = 4v_m^2(1/4 - 1/6) = (1/3)\,v_m^2\,, \tag{14a}$$

$$\Delta\overline{v^2} = \overline{v^2} - \bar{v}^2 = v_m^2(\tfrac{1}{3} - 64/225) = (11/225)\,v_m^2 \simeq (1/20)\,v_m^2\,, \tag{15a}$$

$$\text{r.m.s. } \Delta v \simeq (1/4.5)\,v_m\,. \tag{16a}$$

For both the energy and velocity distribution the r.m.s. spread appears to be about $\frac{1}{4}$ of the maximum value. Thus the spread in the electron bunching corresponds to $2 \times v_m/4 = v_m/2$ rather than v_m. The detailed calculations will now be applied to the geometry of the cathode-ray tube where the photo-electrons are accelerated over a short path L and fly over a long path through the deflection system with uniform velocity.

The time-of-flight spread caused by the initial velocity distribution will be calculated for a uniform acceleration over a distance L and an initial energy $\mathscr{E}$ for the electron. Then

$$E = E_m X/L \tag{17}$$

where E_m is the maximum energy attained by the accelerating electron and

$$v = \sqrt{\frac{2}{M}}\,(E + \mathscr{E})^{\frac{1}{2}}\,, \qquad \text{or} \qquad v = \sqrt{\frac{2}{M}}\,E_m^{\frac{1}{2}}\left(\frac{X}{L} + \frac{\mathscr{E}}{E_m}\right)^{\frac{1}{2}}. \tag{18}$$

The time of flight $T = \int_0^L \mathrm{d}x/v$ and

$$T = \left[\frac{M}{2E_m}\right]^{\frac{1}{2}}\int_0^L \left(\frac{X}{L} + \frac{\mathscr{E}}{E_m}\right)^{-\frac{1}{2}}\mathrm{d}x = \left[\frac{M}{2E_m}\right]^{\frac{1}{2}} 2L\left(\frac{X}{L} + \frac{\mathscr{E}}{E_m}\right)^{\frac{1}{2}}\Bigg|_0^L = T_0\left[\left(1 + \frac{\mathscr{E}}{E_m}\right)^{\frac{1}{2}} - \left(\frac{\mathscr{E}}{E_m}\right)^{\frac{1}{2}}\right]$$

and

$$T = T_0\left[1+\frac{1}{2}\frac{\mathscr{E}}{E_m}-\sqrt{\frac{\mathscr{E}}{E_m}}\right], \tag{19}$$

where

$$T_0 = \frac{2L}{\sqrt{2E_m/M}} \tag{20}$$

is the time of flight for $\mathscr{E}=0$.

For our case $\mathscr{E}_m = \frac{1}{4}$ eV and $E_m = 2.5\cdot 10^4$ eV so that the term linear in $\mathscr{E}/E_m$ is negligible compared to the square root. Therefore

$$T \simeq T_0\left(1-\sqrt{\frac{\mathscr{E}}{E_m}}\right) = T_0\left(1-\frac{v}{V_m}\right), \tag{21}$$

where V_m is the speed corresponding to the energy E_m. The maximum value of the last term is

$$\left[\left(\frac{\mathscr{E}_m}{E_m}\right)\right]^{\frac{1}{2}} = \left[\frac{1}{4\cdot 2.5\cdot 10^4}\right]^{\frac{1}{2}} \simeq \frac{1}{3}\cdot 10^{-2} \tag{22}$$

and the maximum time spread during the acceleration is for $L=1$ cm is

$$\Delta T_m = \frac{T_0}{3}\cdot 10^{-2} = \frac{2}{3}\cdot 10^{-12}\ \mathrm{s}. \tag{23}$$

After the acceleration the electrons emerge with a velocity

$$V = \sqrt{\frac{2}{M}(E_m+\mathscr{E})} = V_m\left(1+\frac{\mathscr{E}}{E_m}\right)^{\frac{1}{2}},$$
$$\simeq V_m\left(1+\frac{1}{2}\frac{\mathscr{E}}{E_m}\right).$$

The time of flight over the distance D from the accelerating electrode to the screen is

$$T_D = \frac{D}{V} = \frac{D}{V_m}\left(1-\frac{1}{2}\frac{\mathscr{E}}{E_m}\right). \tag{25}$$

The maximum deviation from the time of flight corresponding to $\mathscr{E}=0$ is

$$\Delta T_D = \frac{1}{2}\frac{D}{V_m}\frac{\mathscr{E}}{E_m}.$$

For our case $D \sim 50$ cm, $V_m \sim 10^{10}$ cm/s, and $\mathscr{E}/E_m = 10^{-5}$;

$$\Delta T_D = 2.5 \cdot 10^{-14} \text{ s}$$

which is negligible when compared with eq. (23). We therefore conclude that only the time-of-flight spread brought about during the process of acceleration is of importance. This spread is (eq. (21))

$$\Delta T = T_0 \frac{v}{V_m} = \frac{2L}{V_m^2} v = M \frac{L}{E_m} v \,. \tag{21a}$$

For a given v this spread is proportional to L/E_m, *i.e.*, inversely proportional to the accelerating electric field strengths. Since E_m determines the final electron velocity and this has to be tuned to the propagation velocity in the traveling-wave deflecting system, there is probably not much choice in the value of E_m. One possibility of diminishing ΔT is to choose L as small as possible. Another possibility of decreasing the time-of-flight spread is given by the use of a nonuniform accelerating field, such that the electric field strength is made larger in the vicinity of the cathode. This can be achieved by the use of a curved (*e.g.*, spherically shaped) cathode. In the case mentioned above (distance between cathode and accelerating electrode $L = 1$ cm, $E_m = 25$ keV) a curvature of the cathode of 1 cm radius makes the field at the cathode twice the previous value, or 50 kV/cm. This field strength is still tolerable for field emission, which sets in above 100 kV/cm, and it is preferable with respect to break-down as compared to the uniform field with $L = \frac{1}{2}$ cm. The maximum time-of-flight spread would be $\frac{1}{3} \cdot 10^{-12}$ s in this case, permitting higher-frequency operation of the tube.

The influence of the time-of-flight spread on the modulation intensity will now be calculated. If $\mathscr{E} = 0$ the intensity is

$$I = I_0[1 + \cos 2\pi\omega t]$$

at the cathode and

$$I = I_0[1 + \cos 2\pi\omega(t - T_0)]$$

at the accelerating electrode. If $\mathscr{E} \neq 0$, $v \neq 0$, then

$$I = I_0\left[1 + \cos 2\pi\omega\left\{t - T_0\left(1 - \frac{v}{V_m}\right)\right\}\right] . \tag{25}$$

In the case of v variable, the cosine term must be integrated over the velocity

distribution and

$$I(t) = I_0 \left[1 + \int_0^{v_m} \cos 2\pi\omega \left(t' + T_0 \frac{v}{V_m} \right) \varphi(v)\, \mathrm{d}v \right],$$

where $t' = t - T_0$. The second term within the bracket is

$$\int_0^{v_m} \varphi(v) \cos 2\pi\omega \left[t' + T_0 \frac{v}{V_m} \right] \mathrm{d}v = \cos \omega t' \int_0^{v_m} \varphi(v) \cos 2\pi\omega T_0 \frac{v}{V_m}\, \mathrm{d}v -$$

$$- \sin \omega t' \int_0^{v_m} \varphi(v) \sin 2\pi\omega T_0 \frac{v}{V_m}\, \mathrm{d}v = \alpha \cos 2\pi\omega t' - \beta \sin 2\pi\omega t' = \gamma \cos (2\pi\omega t' + \varphi),$$

where

$$\alpha = \frac{4}{v_m^4} \int_0^{v_m} (v_m^2 v - v^3) \cos \omega T_0 \frac{v}{V_m}\, \mathrm{d}v, \tag{26}$$

$$\beta = \frac{4}{v_m^4} \int_0^{v_m} (v_m^2 v - v^3) \sin \omega T_0 \frac{v}{V_m}\, \mathrm{d}v \tag{27}$$

and

$$\gamma = \sqrt{\alpha^2 + \beta^2} \tag{28}$$

is the amplitude of the modulation.

With the substitution

$$x = 2\pi \frac{v\omega T_0}{V_m} = 2\pi\omega \Delta T_m,$$

$$\alpha = \frac{4}{x_m^2} \int_0^{x_m} x \cos x\, \mathrm{d}x - \frac{4}{x_m^4} \int_0^{x_m} x^3 \cos x\, \mathrm{d}x,$$

$$\beta = \frac{4}{x_m^2} \int_0^{x_m} x \sin x\, \mathrm{d}x - \frac{4}{x_m^4} \int_0^{x_m} x^3 \sin x\, \mathrm{d}x.$$

After calculation of the integrals one obtains

$$\alpha = \frac{24}{x_m^3} \sin x_m + \left[\frac{24}{x_m^4} - \frac{8}{x_m^2} \right] \cos x_m - \left[\frac{4}{x_m^2} + \frac{24}{x_m^4} \right],$$

$$\beta = \left[\frac{24}{x_m^4} - \frac{8}{x_m^2} \right] \sin x_m - \frac{24}{x_m^3} \cos x_m.$$

The calculated values of α, β, and γ for several values of x are given in Table I. In Fig. 4 γ is plotted *vs.* x_m. The value $x_m = 2\pi$ corresponds to $\Delta T_m = \frac{2}{3} \cdot 10^{-12}$ s as given in eq. (23) and $\omega = 1.6 \cdot 10^{12}$ Hz.

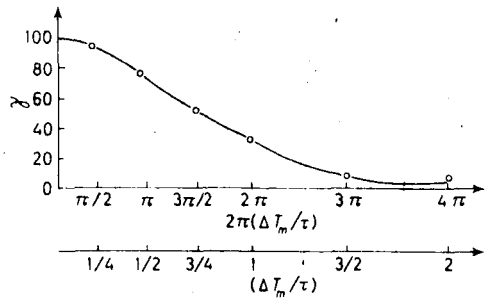

Fig. 4. – Percentage modulation of the electron beam *vs.* $x = 2\pi \Delta T_m/\tau$ where ΔT_m is the maximum time spread for the electrons and ω is the beat frequency.

TABLE I.

	0	$\pi/2$	π	$3\pi/2$	2π	3π	4π
α	1	+ 0.627	— 0.084	— 0.458	— 0.304	+ 0.039	— 0.076
β	0	+ 0.700	+ 0.774	+ 0.321	— 0.097	+ 0.029	— 0.01
γ%	100	93	78	55	31	5	7.6

5·4. *Writing speed limitation.* – The discussion and analysis of the characteristics of the image tube have been based on the performance characteristics of the EG&G Model KR-5 cathode-ray tube [14]. In a similar tube GOLDBERG has reported a writing speed of $3 \cdot 10^{12}$ spot diameter/s [15]. This speed is related to single shot experiments thus the beam intensity required to obtain a photograph in $\frac{1}{3} \cdot 10^{-12}$ s is involved. In our repetitive (current accumulating) experiment the upper limit of the « writing speed » is given by the time-of-flight spread of electrons within the electron focusing and deflecting system. This time-of-flight spread has to be added to the ones calculated in the present analysis for the photoelectron acceleration procedure.

Consider the path length from the accelerating grid to the fluorescent screen to be $D = 2l$ and that an electron can have a lateral displacement d within the aperture of the beam.

The path traversed by the elctron is then $2l'$ rather than $2l$ and the difference in path length will cause a time spread:

$$l' = (l^2 + d^2)^{\frac{1}{2}} = l\left(1 + \frac{d^2}{l^2}\right)^{\frac{1}{2}} \simeq l\left(1 + \frac{1}{2}\frac{d^2}{l^2}\right),$$

$$l' - l = \Delta l = \frac{1}{2}\frac{d^2}{l}$$

and

$$\Delta T = \frac{\Delta l}{V_m}.$$

For the EG&G tube $l \simeq 25$ cm and $d = 0.25$ cm, therefore $\Delta l = 1.25 \cdot 10^{-3}$ cm and

$$\Delta T = \frac{1.25 \cdot 10^{-3} \text{ cm}}{10^{10} \text{ cm/s}} = 1.25 \cdot 10^{-13} \text{ s}.$$

This time spread is less than the time spread in the acceleration process of the photoelectrons (eq. (23)).

Conclusion: The analysis given in this Section shows that the upper frequency limit for the operation of the proposed tube is given by the initial velocity spread of the photoelectrons. If we require a beam modulation amplitude of 30 % or greater, the upper frequency limit of operation is $\sim 1.5 \cdot 10^{12}$ Hz with an accelerating field (at the cathode) of 25 kV/cm and $\sim 3 \cdot 10^{12}$ Hz with a field of 50 kV/cm.

6. – Stability and noise in the frequency measurement.

The accuracy in the measurement of the frequency

$$\pm \mu = \omega - n\Omega$$

is limited by the fluctuations in ω, Ω, and by noise current.

Since the optical frequencies ν_1 and ν_2 are derived from two different oscillations (resulting from two different atomic transitions) of the same cavity, the fluctuations in ν_1 and ν_2 are correlated. By neglecting small nonlinear effects of mode pulling [16]

$$\nu_1 = n_1 \frac{c}{2L}$$

and

$$\nu_2 = n_2 \frac{c}{2L},$$

where n_1 and n_2 are integers. Therefore

$$\nu_1 - \nu_2 = \omega = (n_1 - n_2) \frac{c}{2L}$$

and for a small change δL

$$\frac{\delta \nu_1}{\nu_1} = \frac{\delta \nu_2}{\nu_2} = \frac{\delta \omega}{\omega} = \frac{\delta L}{L}$$

or

$$\delta\omega \simeq \frac{\omega}{\nu}\,\delta\nu\,, \tag{29}$$

where ν is either one of the optical frequencies. Thus, the fluctuation in ω is diminished in proportion to the ratio of the beat frequency and the optical frequency. Taking $\Delta\nu \sim \pm 5$ kHz (which appears to be the present long-term stability with lasers [17]) $\Delta\omega \sim \pm 15$ Hz for $\omega \sim 10^{12}$ Hz.

The stability of the driving frequency Ω can be made 1 Hz without great effort. Since Ω is frequency multiplied by the mask number n in the experiment and $n \sim 10^2$, the major fluctuation in μ is expected to come from the instability in Ω rather than from the laser. Both instabilities result in the precision of ω to about one part in 10^{10}.

The probability character of the photoelectron emission results in shot noise. It can be shown by a qualitative argument, that the frequency instability in the measurement of μ, caused by noise, is much lass than one part in 10^{10}.

In the frequency measurement, the output current I is a function of μ. The sensitivity of the measurement is proportional to the slope $S = \mathrm{d}I(\mu)/\mathrm{d}\mu$. Therefore, an uncertainty in the current δI results in an uncertainty

$$\delta\mu = \frac{\delta I(\mu)}{S}\,. \tag{30}$$

The bandwidth of the filter, $\Delta\mu_f$, must be larger than the bandwidth $\Delta\mu$ given by the frequency fluctuation of the input signal. A reasonable value for the filter bandwidth is

$$\Delta\mu_f \simeq 10\,\Delta\mu\,.$$

An upper limit for the slope S can be taken as

$$S = \frac{I(\mu)}{\Delta\mu_f}$$

and, from eq. (30),

$$\delta\mu = \frac{\delta I}{I}\,\Delta\mu_f\,. \tag{31}$$

Using the shot noise formula

$$\overline{\delta I^2} = 2eI\,\Delta\mu_f$$

we obtain

$$\delta\mu = \sqrt{\frac{2e(\Delta\mu f_f)^3}{I}}\,. \tag{32}$$

If we consider a 20 microwatt power output for each laser line and a photoefficiency of 10^{-4} at 1.1 μ (S1 photosurface) then $I = 1.6 \cdot 10^{-9}$ A. With a filter

bandwidth $\Delta\mu_f = 10^3$ Hz,

$$\delta\mu \simeq 0.5 \text{ Hz} ,$$

which is less than 1/100 of the fluctuation $\Delta\mu = 100$ Hz caused by the microwave frequency instability Ω.

7. – Summary.

It was shown in Sect. 3 that a measurement of the wave-number separation $K \simeq 40$ cm^{-1} could be made with a precision of one part in 10^8 using a Fabry-Perot interferometer of 1.5 meter length.

It was shown in Sect. 5 and 6 that the measurement of the beat frequency $\omega = 10^{12}$ Hz (corresponding to $K = 40$ cm^{-1}) is feasible and its precision could be made one part in 10^{10}.

Therefore, a measurement of the velocity of light with a precision of one part in 10^8 could be done in a laboratory of conventional size.

* * *

It is a pleasure to thank P. L. BENDER, R. D. HUNTOON, K. G. KESSLER, G. G. LUTHER, W. C. MARTIN, and W. G. SCHWEITZER for several illuminating discussions.

APPENDIX

Departures from the ideal conditions of modulation.

In the treatment of the beat experiment one has to take into account that:

1) the Z-modulation of the cathode-ray beam with the frequency ω is not pure harmonic;

2) the transparency function of the mask is not pure harmonic.

Such departures from the ideal case can easily be accounted for by repladin, the cosine terms in eqs. (4) and (5) by the Fourier expansions of the modulation functions. Then

$$I = I_0 \Big[\sum_{k=0}^{\infty} a_k \cos(2\pi k\omega t + \varphi_k)\Big] \Big[\sum_{l=0}^{\infty} a_l \cos(2\pi l\Omega t + \varphi_l)\Big] . \tag{A.1}$$

A general remark can be made about the amplitude a_k. Since it is planned to measure the very highest frequencies detectable in the experiment, the higher harmonics k of ω will not be well resolved. Thus beyond $k = 0$ and $k = 1$, the a_k amplitudes will rapidly decrease with increasing k.

There are several effects which would give rise to the anharmonicity of the transparency function. Such effects are, for example,

a) the wave structure of the mask is distorted,

b) the mask transparency may not be sinusoidal.

In using the mask in the high-frequency-beat experiment, errors appear if

c) the fluorescent screen illumination is not linear with beam intensity,

d) the beam deflection is not exactly centered around the center of the mask,

e). the amplitude of the beam deflection does not eactly match the size of the mask,

f) the photomultiplier does not give a uniform response to the full extension of the kask,

g) the X-deflection of the beam is not sinusoidal in time, etc.

It is important to point out that all the imperfections *a*), ..., *g*), and others, can only lead to a simple line spectrum given by the Fourier expansion of eq. (A.1) with the frequencies $l\Omega$ and amplitudes a_l. This can be seen in the following way. Let the transparency (as seen by the photomultiplier) be any function $F(x)$ of the position co-ordinate in the mask. Now the position co-ordinate of the moving beam spot will be a periodic function, say $\varphi(t)$, of the time, *i.e.*,

$$\varphi(t + T) = \varphi(t) ,$$

where $T = 1/\Omega$. Thus $F(x) = F[\varphi(t)]$ is a periodic function of the time with the period T.

Therefore, imperfections in the mask and in its use can be characterized by the statement that the mask number n splits up into a spectrum of integers l. The breadth of this spectrum depends on the imperfections, but certainly the values of l which are near n will be the most significant in the experiment. Therefore n, for which the mask is prepared, still retains its significance and will further be called the mask number.

In contrast to the single doublet of the ideal experiment, the harmonics in eq. (A.1) lead to a multiplicity of beats in the output of the phototube. They are characterised by the frequencies $k\omega - l\Omega$. In case the low-frequency filter μ is used, one obtains

$$k\omega - l\Omega = \pm\mu . \tag{A.2}$$

1) First the case $K = 1$ is treated. For each value l a doublet

$$\Omega_{l+} = \frac{\omega + \mu}{l} , \qquad \Omega_{l-} = \frac{\omega - \mu}{l} , \tag{A.3}$$

is obtained with the center $\Omega_l = \omega/l$ and doublet separation $2\mu/l$. The centers of the l-th and $(l+1)$-th doublet are separated by

$$\Omega_l - \Omega_{l+1} = \Omega_l \frac{1}{l+1} = \Omega_{l+1} \frac{1}{l} ,$$

consequently

$$l = \frac{\Omega_{l+1}}{\Omega_l - \Omega_{l+1}}$$

and also

$$l = \frac{\Omega_{l-1}}{\Omega_{l-1} - \Omega_l}. \tag{A.4}$$

Thus eq. (A.4) gives means for the determination of the « order number » l of a doublet by measuring the frequencies of the doublet centers and using the « order separations », $\Omega_l - \Omega_{l+1}$ or $\Omega_{l-1} - \Omega_l$, of neighboring doublets.

The knowledge of the order number l determines the high frequency to be measured as

$$\omega = l\Omega_l \tag{A.5}$$

without ambiguity.

The knowledge of the mask number n facilitates location of the doublets when arranging an experiment. For example if $n = 100$, the doublet separation is expected to be $\sim 1\,\%$ of 2μ and the order separation $\sim 1\,\%$ of Ω.

2) For $k > 1$ only the beats between $k\omega$ and $l' \sim kl\Omega$ can result in low frequencies equal to μ. For these

$$\omega - l'\Omega = \pm \frac{\mu}{k}. \tag{A.6}$$

These lines appear *within* the doublets given generally by eq. (A.3) and represent lines which are at the distances $\pm\mu/2$, $\pm\mu/3$, $\pm\mu/4$, ... from the center. It is to be expected that their amplitudes decrease rapidly with increasing k. If they can be detected they can be utilized as additional information for the determination of the doublet centers.

Model experiments.

With the mask of Fig. 2 model experiments have been performed with

$$\omega = 10^7 \text{ Hz}, \qquad \mu = 2 \cdot 10^4 \text{ Hz}.$$

Ω was slowly varied around 10^5 Hz. The output of the filter was viewed on an oscilloscope and it also was introduced through a diode demodulator into a recorder. The frequency Ω was read on a frequency counter. The recorder output as a function of Ω is shown in Fig. 5. The doublets appear at the frequencies as expected. The separation in the doublets is

$$\sim \frac{2 \cdot 2 \cdot 10^4}{100} = 400 \text{ Hz}$$

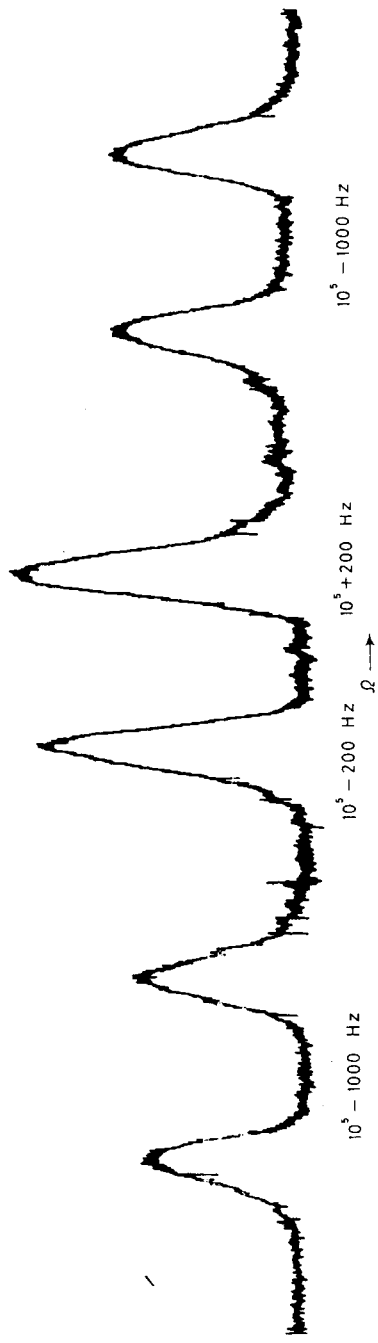

Fig. 5. – Recorder output as a function of Ω. Doublet separation is 400 Hz. Separation between neighboring doublets is 10^3 Hz.

and the separation between neighboring doublets is

$$\sim \frac{10^5}{100} = 10^3 \text{ Hz}.$$

No additional lines within the doublets (corresponding to $k > 1$) could be detected in the experiment.

REFERENCES

[1] A. JAVAN, W. R. BENNETT jr. and D. R. HERRIOT: *Phys. Rev. Lett.*, **6**, 106 (1961).

[2] K. F. NEFFLEN, T. MOROHUMA, T. KLUCHER and T. LAWRENCE: to be published.

[3] A. JAVAN: *Proc. of the Third International Conference on Quantum Electronics* (Paris, 1963); T. S. JASEJA, A. JAVAN and C. H. TOWNES: *Phys. Rev. Lett.*, **10**, 165 (1963).

[4] A. T. FORRESTER, R. A. GUDMUNDSEN and P. O. JOHNSON: *Phys. Rev.*, **99** 1691 (1955).

[5] See for example: P. JACQUINOT and C. DUFOUR: *Journ. Recherches C.N.R.S.*, 2, 91 (1948); C. F. BRUCE and R. M. HILL: *Astral. Journ. Phys.*, **14**, 61 (1961).

[6] R. L. BARGER and K. G. KESSLER: *Journ. Opt. Soc. Am.*, **50**, 651 (1960); W. G. SCHWEITZER: to be published.

[7] R. A. PAANANEN (*Proc. I.R.E.*, **50**, 2115 (1962)) has measured the passive bandwidth of a one-meter laser interferometer to be 0.3 MHz. This measurement implies a finesse $\simeq 500$.

[8] The 1.207, 1.199, 1.161 and 1.118 μm lines were reported in ref. [1]. The 1.139, 1.084 and 1.080 μm lines were reported by R. A. MCFARLANE, C. K. N. PATEL, W. R. BENNETT jr. and W. L. FAUST: *Proc. I.R.E.*, **50**, 2111 (1962). The 1.140 and 1.160 μm lines were reported by J. D. RIGDEN and A. D. WHITE: *Proc. of the Third International Conference on Quantum Electronics* (Paris, 1963) under the condition that the 6328 Å line was used to suppress the 1.53 μm line which competes with the two above mentioned transitions.

[9] This averaging is permissible since the optical frequencies ν_1 and ν_2 are washed out by the velocity spread of the photoelectrons discussed in Sect. 5.3.

[10] P. S. PERSHAN and N. BLOEMBERGEN: *Appl. Phys. Lett.*, **2**, 117 (1963).

[11] L. A. DUBRIDGE: *Phys. Rev.*, **43**, 727 (1933).

[12] C. L. HENSHAW: *Phys. Rev.*, **52**, 854 (1937).

[13] There is some ambiguity as to the value of the work function Φ. We have taken $\Phi = \frac{3}{4}$ V as a lower limit representing the maximum possible spread in the electron energy distribution function.

[14] E. G. & G. Tech. Memo no. B-391 (October 1962).

[15] J. GOLDBERG: *Conference on Fast Pulse Techniques in Nuclear Counting* (Berkeley, Calif., 1959).

[16] W. R. BENNETT jr.: *Applied Optics Supplement on Optical Masers* (December 1962).

[17] T. S. JASEJA, A. JAVAN and C. H. TOWNES (*Phys. Rev. Lett.*, **10**, 165 (1963)) have demonstrated a short term (1 to 2 s) stability of this order using two free running lasers. P. RABINOWITZ, J. LA TOURETTE and G. GOULD (*Proc. I.E.E.E.*, **51**, 857 (1963)) have achieved a tracking accuracy of this order with two lasers using optical heterodyne detection.

APPENDIX II

Dispersion Characteristics of the 1.15μ He-Ne Laser Line*

H. S. Boyne
M. M. Birky
W. G. Schweitzer, Jr.
Atomic Physics Division, National Bureau of Standards, Washington, D. C.

An experimental investigation of the dispersion characteristics of the 1.15μ He-Ne laser line ($2s_2$-$2p_4$) due to mode pushing effects[1] shows that the predicted behavior of the frequency deviation $\delta\nu$ resulting from a variation in the relative inversion density above threshold is complicated by a neighboring neon absorption transition. In order to investigate this perturbation we have obtained dispersion curves by modulating the inversion density in the following ways:

a) Power modulation of the plasma discharge.[2]

b) Modulation of $2s_2$ level in neon by optically pumping the 2^3S He level with the $2^3S \rightarrow 2^3P$ 1.083μ He line.

c) Modulation of $2p_4$ level of neon by optically pumping it with the $1s_4$-$2p_4$ .6096μ line and the $1s_5 \rightarrow 2p_4$ .5944μ line in neon.

The experimental arrangement used for observing the frequency dispersion curves is schematically represented in Figure 1. Two 1.15μ He-Ne lasers of 1 meter length and flat plate internal mirror construction[3] were locked together at a frequency difference of 10.7 MHz. Since the dominant frequency fluctuation rate of the unlocked

*This research was supported in part by NASA Goddard Space Flight Center, Contract No. S-49296(G).

lasers was a few hundred cycles and below, a servo loop gain which falls to unity at 1 kHz was used to lock system. The resulting beat note had a spectral width of $\sim$ 4 kHz.[4]

The modulation of the inversion density δN which results in the frequency deviation $\delta\nu$ is accomplished by modulating the rf power or by optical pumping as described below. The resulting frequency deviation is detected at the discriminator output. This signal is then fed into a phase sensitive detector tuned to the modulation frequency and displayed on the y axis of an x-y recorder. The resulting dispersion curve is obtained by slowly sweeping the length of both lasers magnetostrictively and applying the sweep voltage to the x axis of the recorder. The frequency deviation $\delta\nu$ depends on the difference between the laser frequency and the frequency of the atomic line center and is given by[1]

$$\delta\nu_n \simeq 1/2\ \frac{\nu}{Q}\left\{\left[1 - \frac{2\gamma_{ab}}{\sqrt{\pi}Ku}\right]\frac{\gamma_{ab}(\Omega_n-\omega)}{2\gamma_{ab}^2+(\Omega_n-\omega)^2} - \frac{2(\Omega_n-\omega)}{\sqrt{\pi}Ku}\right\}\delta N$$

where the first term in the bracket arises from the variation of frequency pushing with the depth of the hole burned in the gain curve and the second term is a linear approximation to the dispersion of the normal gain curve. $\frac{\nu}{Q_n}$ is the passive cavity bandwidth of the laser, $\gamma_{ab/\pi}$ is the natural width of the laser transition, Ku is proportional to the Doppler width, ν_n is the laser frequency, Ω_n is the cavity frequency, ω is the frequency of the transition at the line center and δN is the relative excitation above oscillation threshold. This equation is valid to first order in $\gamma_{ab/Ku}$

and $\frac{\Omega_n - \omega}{Ku}$ which are of order 0.15 for this experiment. $\delta\nu_n$ approaches zero linearly as $(\Omega_n - \omega) \rightarrow 0$ provided there are no neighboring transitions whose dispersion contributes to $\delta\nu$. Such a contribution is evident in all the dispersion curves shown in Figure 2. Since these curves were taken using 1 meter lasers in single mode operation, the maximum relative excitation above threshold δN_{max} is restricted to 1%-2%. Therefore with $\gamma_{ab/\tau} \simeq 90$ MHz and $\frac{\nu}{Q_n} \simeq 1.5$ MHz, $(\Omega_n - \omega) \approx 45$ MHz, $\delta\nu_{max} \simeq 4$ kHz. In each of the curves in Figure 2 the modulation of the relative excitation was approximately 5% of δN_{max} thereby giving a $\delta\nu \simeq 200$ Hz. γ_{ab} was obtained by solving equation 1 for the extreme values of $(\Omega_n - \omega)$. Assuming Ku = 500 MHz, then $\Delta\nu_n = \gamma_{ab/\tau} = 90$ MHz.

Figure 2a shows the results obtained by modulating the rf power to the discharge at a 4 kHz rate, thus modulating the relative excitation of the $2s_2$ and $2p_4$ levels. With rf modulation there is a background of ≈ 650 Hz on the observed $\delta\nu$ which is due to the dispersion of the plasma electrons and to other nearby neon lines, principally the $2p_7$-$2s_4$ 1.15232μ absorption line.

Curve 2b was obtained by optically pumping the 2^3S-2^3P 1.083μ He line. Since the principal excitation mechanism of the 2s neon levels is by energy exchange with the 2^3S metastable helium, the 2^3S He $\rightarrow$ 2s Ne exchange rate is modulated (Figure 3). This type of modulation minimizes the dispersion effect of the electron plasma but still affects the $2s_4$-$2p_4$ transition and causes a shift of

$\sim$ 250 Hz in $\delta\nu$ at the line center. The optical pumping was accomplished by modulating the intensity of a He Geissler tube placed about 4 inches from and parallel to the laser discharge tube (Figure 1). The radiation from the lamp was confined to the region around the laser discharge by diffuse reflectors. This method of light collection was found superior to a lens system. The intensity of the lamp was modulated at a 4 kHz rate. This produced a modulation of approximately .05 δN_{max} which is limited by the intensity of the lamp.

Curve 2c was obtained by modulating the population density of the lower 2p levels of neon with a Ne Geissler tube replacing the He lamp in the configuration described above (Figure 3). The neon lamp modulates both the $2p_4$ and $2p_7$ levels which contribute a background to $\delta\nu$ as seen in Figure 3c. However, the effect of the $2s_4$-$2p_7$ transition is considerably reduced. It is interesting to note the results of attempts to isolate specific Ne lines. A series of Corning high frequency sharp cutoff filters was used to isolate the $1s_2$-$2p_4$ transition. Optical pumping with this line had a negligible effect on the modulation of the $2p_4$ level population.

Curve 2d was obtained in a manner similar to 2c except that narrow bandpass filters were used to discriminate against the levels connecting the 1s levels to the $2p_7$ level. The relative intensities of the pertinent lines both with and without the narrow bandpass filters are as follows:

Transition	Unfiltered Ne Lamp	Narrow Band Filtered Ne
$1s_2$-$2p_7$	6	0
$1s_3$-$2p_7$	1	0
$1s_4$-$2p_7$	2	.25
$1s_5$-$2p_7$	0.6	.25
$1s_2$-$2p_4$	3	0
$1s_4$-$2p_4$	1	1
$1s_5$-$2p_4$	0.7	0.7

It is seen that curve 2d more nearly approaches the result predicted by Equation 1. There is some asymmetry in the dispersion curve which is conceivably due to a pressure induced asymmetry in the laser transition.[5]

In all three modulation schemes the effect of modulating the relative excitation also causes a modulation in the output power of the laser line. In the case of the rf power modulation the relative excitation increases with increasing power. However, in both the He and Ne optical pumping an increase in the intensity of the lamp causes the relative excitation above threshold to decrease. This corresponds to absorption of the pumping radiation.

The dispersion resulting from modulation of the inversion density by optical pumping with neon can be used to develop an error signal for stabilizing the 1.15μ line to the atomic line center.[6] This type of stabilization should be equally effective for the .6328μ $3s_2$-$2p_4$ laser line.

It is a pleasure to acknowledge helpful discussions with Z. Bay and G. G. Luther.

References

1) W. E. Lamb, Jr., Phys. Rev. 134, A1429 (1964): W. R. Bennett, Jr. Quantum Electronics III eds.; P. Grivet and N. Bloembergen (Columbia University Press, New York 1964) p. 441 ff.

2) W. R. Bennett, Jr., S. F. Jacobs, J. T. LaTourrette, and P. Rabinowitz, Appl. Phys. Letters 5, 56 (1964) have described this method of modulation for stabilizing the He-Ne 3.39μ laser line.

3) W. R. Bennett, Jr. and P. J. Kindlmann, Rev. Sci. Instr. 33, 601 (1962).

4) This heterodyne scheme is similar to that described by P. Rabinowitz, J. T. LaTourrette, and G. Gould, Proc. IRE 51, 857 (1963).

5) A. Szöke, Bull Am. Phys. Soc. 9, 65 (1964); K. Shimoda and A. Javan, J. Appl. Phys. 36, 718 (1964).

6) See W. R. Bennett, Jr., Ref. 1 and 2.

FIGURE CAPTIONS

Figure 1. Deflection system power supply

Figure 2. Sound shielded room showing 1 meter lasers used in beat experiments

Figure 3. Typical frequency spectra of the beat notes between two lasers

Figure 4. Plot of output power vs. frequency of the He-Ne laser

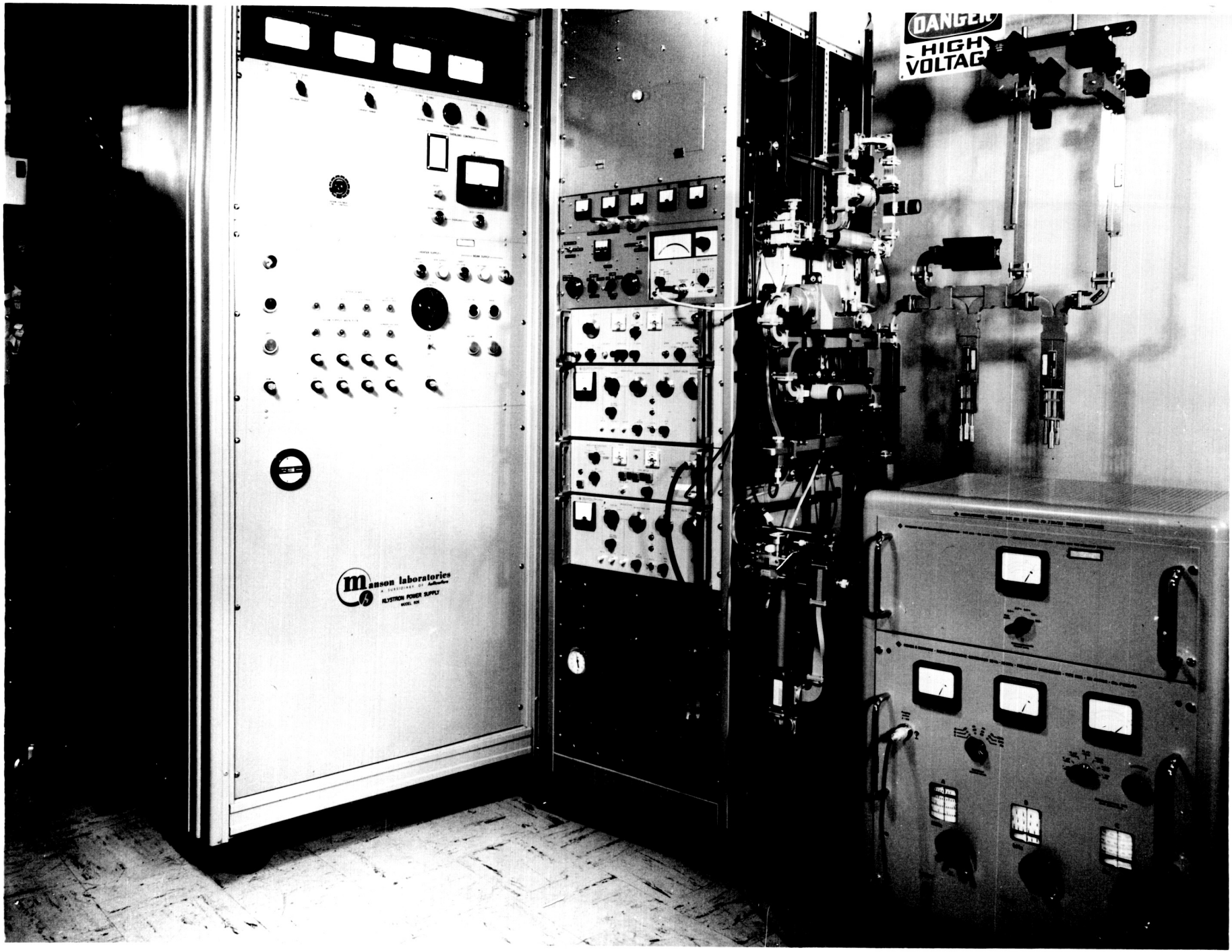
DANGER
HIGH
VOLTAG
manson laboratories
KLYSTRON POWER SUPPLY

Figure 1

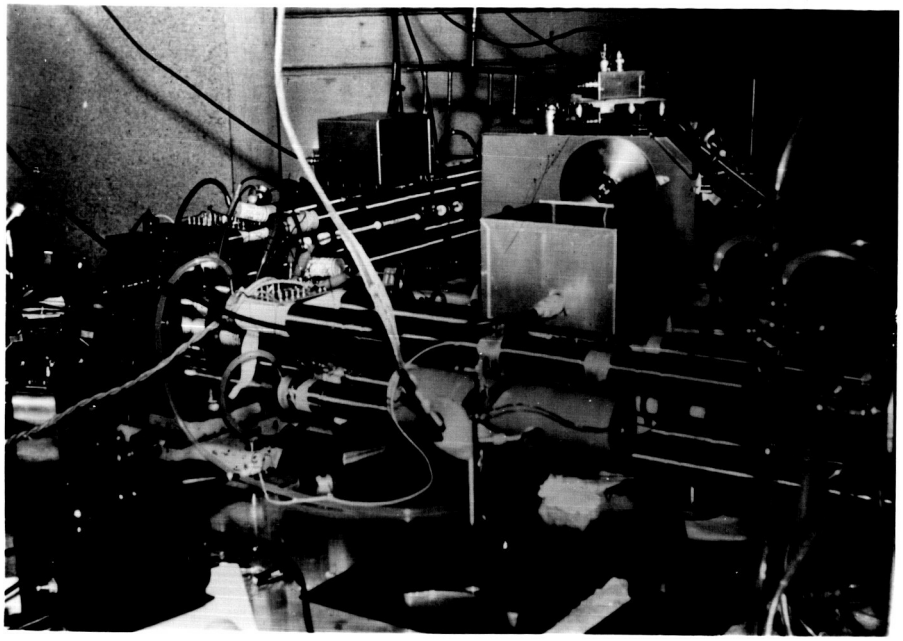

Figure 2

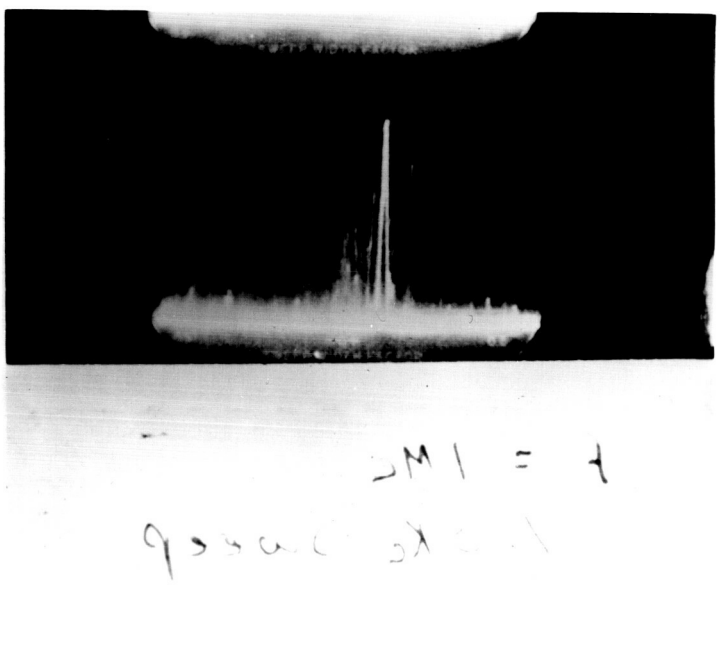

Figure 3

Figure 4

Reprinted from
Volume 7, Number 3 APPLIED PHYSICS LETTERS 1 August 1965

DISPERSION CHARACTERISTICS OF THE 1.15-μ He-Ne LASER LINE[1]

H. S. Boyne, M. M. Birky, and W. G. Schweitzer, Jr.
Atomic Physics Division
National Bureau of Standards
Washington, D. C.
(Received 30 April 1965; in final form 3 June 1965)

(Ne absorption transition; E/T)

An experimental investigation of the dispersion characteristics of the 1.15-μ He-Ne laser line ($2s_2$–$2p_4$) due to mode pushing effects[2] shows that the predicted behavior of the frequency deviation $\delta\nu$ resulting from a variation in the relative inversion density above threshold is complicated by a neighboring neon absorption transition. In order to investigate this perturbation we have obtained dispersion curves by modulating the inversion density in the following ways:

1. power modulation of the plasma discharge.[3]
2. modulation of $2s_2$ level in neon by optically pumping the 2^3S He level with the $2^3S \rightarrow 2^3P$ 1.083-μ He line.
3. modulation of $2p_4$ level of neon by optically pumping it with the $1s_4 - 2p_4$ 0.6096-μ line and the $1s_5 \rightarrow 2p_4$ 0.5944-μ line in neon.

The experimental arrangement used for observing the frequency dispersion curves is schematically represented in Fig. 1. Two 1.15-μ He-Ne

lasers of 1-meter length and flat-plate internal mirror construction[4] were locked together at a frequency difference of 10.7 MHz. Since the dominant frequency fluctuation rate of the unlocked lasers was a few hundred cycles and below, a servo loop gain which falls to unity at 1 kHz was used to lock system. The resulting beat note had a spectral width of ~4 kHz.[5]

The modulation of the inversion density δN which results in the frequency deviation $\delta\nu$ is accomplished by modulating the rf power or by optical pumping as described below. The resulting frequency deviation is detected at the discriminator output. This signal is then fed into a phase-sensitive detector tuned to the modulation frequency and displayed on the y axis of an x-y recorder. The resulting dispersion curve is obtained by slowly sweeping the length of both lasers magnetostrictively and applying the sweep voltage to the x axis of the recorder. The frequency deviation $\delta\nu$ depends on the difference between the laser frequency and the frequency of the atomic line center and is given by[2]

$$\delta\nu_n \cong \frac{1}{2}\frac{\nu}{Q}\left\{\left[1-\frac{2\gamma_{ab}}{\sqrt{\pi Ku}}\right]\frac{\gamma_{ab}(\Omega_n-\omega)}{2\gamma_{ab}^2+(\Omega_n-\omega)^2} - \frac{2(\Omega_n-\omega)}{\sqrt{\pi Ku}}\right\}\delta N\,, \qquad (1)$$

where the first term in the bracket arises from the variation of frequency pushing with the depth of the hole burned in the gain curve and the second term is a linear approximation to the dispersion of the normal gain curve. ν/Q_n is the passive cavity bandwidth of the laser, $\gamma_{ab/\pi}$ is the natural width of the laser transition, Ku is proportional to the Doppler width, ν_n is the laser frequency, Ω_n is the cavity frequency, ω is the frequency of the transition at the line center, and δN is the relative excitation above oscillation threshold. This equation is valid to first order in $\gamma_{ab/Ku}$ and $(\Omega_n-\omega)/Ku$ which are of order 0.15 for this experiment. $\delta\nu_n$ approaches zero linearly as $(\Omega_n-\omega)\rightarrow 0$ provided there are no neighboring transitions whose dispersion contributes to $\delta\nu$. Such a contribution is evident in all the dispersion curves shown in Fig. 2. Since these curves were taken using 1-meter lasers in single-mode operation, the maximum relative excitation above threshold $\delta N_{\max}$ is restricted to 1%–2%. Therefore with $\gamma_{ab/\pi}\simeq 90$ MHz and $\nu/Q_n\simeq 1.5$ MHz, $(\Omega_n-\omega)=45$ MHz, $\delta\nu_{\max}\simeq 4$ kHz. In each of the curves in Fig. 2 the modulation of the relative excitation was approximately 5% of $\delta N_{\max}$ thereby giving a $\delta\nu\simeq 200$ Hz. γ_{ab} was obtained by

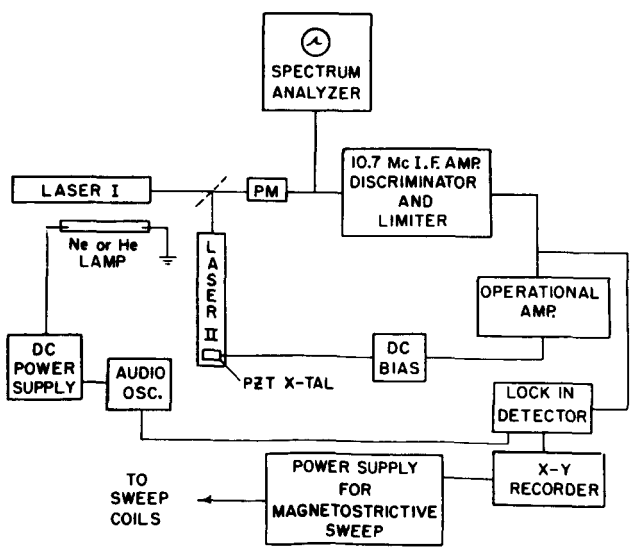

Fig. 1. Block diagram of the experimental arrangement used for observing the frequency dispersion.

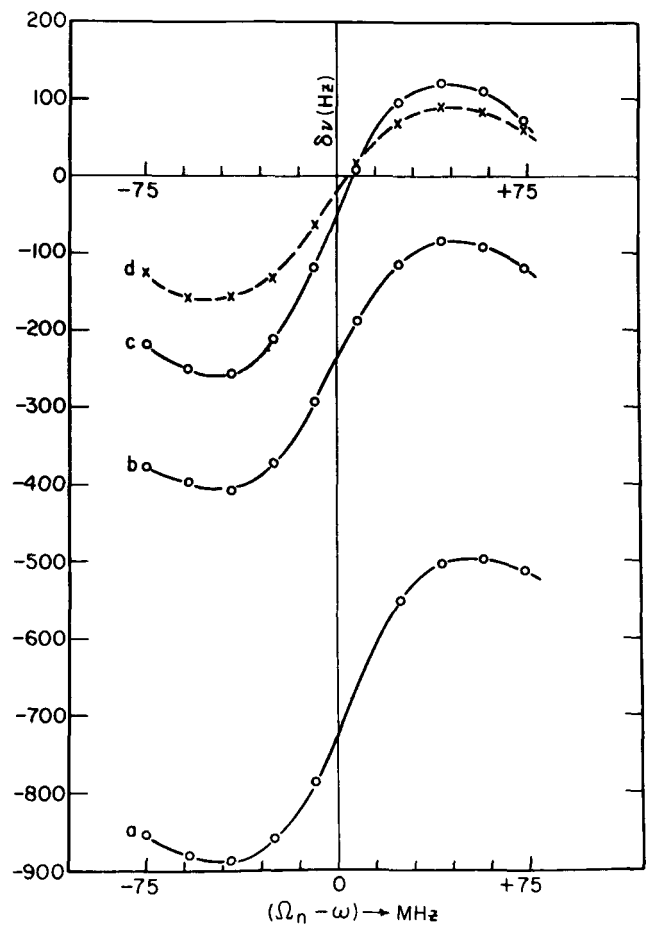

Fig. 2. Experimental dispersion curves: (*a*) dispersion resulting from rf power modulation, (*b*) dispersion resulting from He optical pumping, (*c*) dispersion resulting from unfiltered Ne optical pumping, (*d*) dispersion resulting from filtered Ne optical pumping.

solving Eq. (1) for the values of $(\Omega - \omega)$ at the extremes of the dispersion. Assuming $Ku = 500$ MHz, then $\Delta\nu_n = \gamma_{ab/\pi} = 90$ MHz.

Figure 2*a* shows the results obtained by modulating the rf power to the discharge at a 4-kHz rate, thus modulating the relative excitation of the $2s_2$ and $2p_4$ levels. With rf modulation there is a background of ≈650 Hz on the observed $\delta\nu$ which is due to the dispersion of the plasma electrons and to other nearby neon lines, principally the $2p_7 - 2s_4$ 1.15282-μ absorption line.

Curve 2*b* was obtained by optically pumping the 2^3S-2^3P 1.083-μ He line. Since the principal excitation mechanism of the 2*s* neon levels is by energy exchange with the 2^3S metastable helium, the 2^3S He → 2*s* Ne exchange rate is modulated (Fig. 3). This type of modulation minimizes the dispersion effect of the electron plasma but still affects the $2s_4$-$2p_4$ transition and causes a shift of ~250 Hz in $\delta\nu$ at the line center. The optical pumping was accomplished by modulating the intensity of an He Geissler tube placed about 4 in. from and parallel to the laser discharge tube (Fig. 1). The radiation from the lamp was confined to the region around the laser discharge by diffuse reflectors. This method of light collection was found superior to a lens system. The intensity of the lamp was modulated at a 4-kHz rate. This produced a modulation of approximately 0.05 δN_{max} which is limited by the intensity of the lamp.

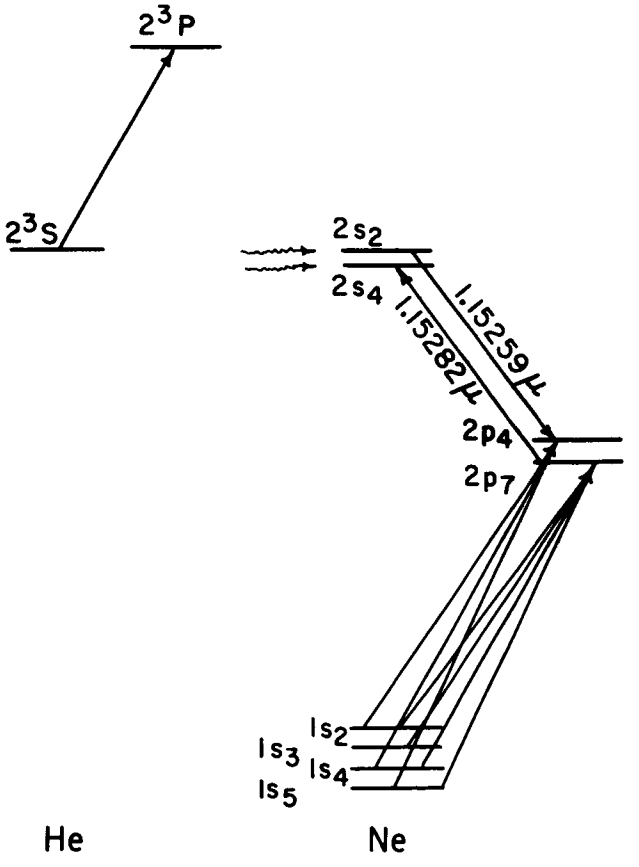

Fig. 3. Partial energy-level diagram of the pertinent He and Ne levels involved in the optical pumping method.

Curve 2*c* was obtained by modulating the population density of the lower 2*p* levels of neon with a Ne Geissler tube replacing the He lamp in the configuration described above (Fig. 3). The neon lamp modulates both the $2p_4$ and $2p_7$ levels which contribute a background to $\delta\nu$ as seen in Fig. 3*c*. However, the effect of the $2s_4$-$2p_7$ transition is considerably reduced. It is interesting to note the results of attempts to isolate specific Ne lines. A series of Corning high-frequency sharp-cutoff filters was used to isolate the $1s_2$-$2p_4$ transition. Optical pumping with this line had a negligible effect on the modulation of the $2p_4$ level population.

Curve 2*d* was obtained in a manner similar to 2*c* except that narrow bandpass filters were used to discriminate against the levels connecting the 1*s* levels to the $2p_7$ level. The relative intensities of the pertinent lines both with and without the narrow bandpass filters are as follows:

Transition	Unfiltered Ne Lamp	Narrow Band Filtered Ne
$1s_2$-$2p_7$	6	0
$1s_3$-$2p_7$	1	0
$1s_4$-$2p_7$	2	.25
$1s_5$-$2p_7$	0.6	.25
$1s_2$-$2p_4$	3	0
$1s_4$-$2p_4$	1	1
$1s_5$-$2p_4$	0.7	0.7

It is seen that curve 2*d* more nearly approaches the result predicted by Eq. (1). There is some asymmetry in the dispersion curve which is conceivably due to a pressure-induced asymmetry in the laser transition.[6]

In all three modulation schemes the effect of modulating the relative excitation also causes a modulation in the output power of the laser line. In the case of the rf power modulation the relative excitation increases with increasing power. However, in both the He and Ne optical pumping an increase in the intensity of the lamp causes the relative excitation above threshold to decrease. This corresponds to absorption of the pumping radiation.

The dispersion resulting from modulation of the inversion density by optical pumping with neon can be used to develop an error signal for stabilizing the 1.15-μ line to the atomic line center.[7] This type of stabilization should be equally effective for the 0.6328-μ $3s_2$-$2p_4$ laser line.

It is a pleasure to acknowledge helpful discussions with Z. Bay and G. G. Luther.

[1]This research was supported in part by NASA Goddard Space Flight Center, Contract No. S-49296(G).

[2]W. E. Lamb, Jr., *Phys. Rev.* **134,** A1429 (1964): W. R. Bennett, Jr., Quantum Electronics III, eds. P. Grivet and N. Bloembergen (Columbia University Press, New York, 1964) p. 441 *ff.*

[3]W. R. Bennett, Jr., S. F. Jacobs, J. T. LaTourrette, and P. Rabinowitz, *Appl. Phys. Letters* **5,** 56 (1964), have described this method of modulation for stabilizing the He-Ne 3.39-μ laser line.

[4]W. R. Bennett, Jr., and P. J. Kindlmann, *Rev. Sci. Instr.* **33,** 601 (1962).

[5]This heterodyne scheme is similar to that described by P. Rabinowitz, J. T. LaTourrette, and G. Gould, *Proc. IEEE* **51,** 857 (1963).

[6]A. Szöke, *Bull. Am. Phys. Soc.* **9,** 65 (1964); K. Shimoda and A. Javan, *J. Appl. Phys.* **36,** 718 (1964).

[7]See W. R. Bennett, Jr., refs. 1 and 2.